Title

A protein aggregation platform that distinguishes oligomers from amyloid fibrils.

Journal

Analyst, 148(10)

Authors

Zhang, Amy
Portugal Barron, Diana
Chen, Erica
et al.

Publication Date

2023-05-16

DOI

10.1039/d3an00487b

Peer reviewed

HHS Public Access

Author manuscript

Analyst. Author manuscript; available in PMC 2024 May 16.

Published in final edited form as:

Analyst. ; 148(10): 2283–2294. doi:10.1039/d3an00487b.

A protein aggregation platform that distinguishes oligomers from amyloid fibrils

Amy Zhang,

Diana Portugal Barron,

Erica W. Chen,

Zhefeng Guo*

Department of Neurology, Brain Research Institute, David Geffen School of Medicine, University of California, Los Angeles, Los Angeles, CA, USA

Abstract

Deposition of aggregated proteins is a pathological feature in many neurodegenerative disorders such as Alzheimer's and Parkinson's. In addition to insoluble amyloid fibrils, protein aggregation leads to the formation of soluble oligomers, which are more toxic and pathogenic than fibrils. However, it is challenging to screen for inhibitors targeting oligomers due to the overlapping processes of oligomerization and fibrillization. Here we report a protein aggregation platform that uses intact and split TEM-1 β-lactamase proteins as reporters of protein aggregation. The intact β-lactamase fused with an amyloid protein can report the overall protein aggregation, which leads to loss of lactamase activity. On the other hand, reconstitution of active β-lactamase from the split lactamase construct requires the formation of amyloid oligomers, making the split lactamase system sensitive to oligomerization. Using Aβ, a protein that forms amyloid plaques in Alzheimer's disease, we show that the growth curves of bacterial cells expressing either intact or split lactamase-Aβ fusion proteins can report changes in the Aβ aggregation. The cell lysate lactamase activity assays show that the oligomer fraction accounts for 20% of total activity for the split lactamase-Aβ construct, but only 3% of total activity for the intact lactamase-Aβ construct, confirming the sensitivity of the split lactamase to oligomerization. The combination of the intact and split lactamase constructs allows the distinction of aggregation modulators targeting oligomerization from those targeting overall aggregation. These low-cost bacterial cell-based and biochemical assays are suitable for high-throughput screening of aggregation inhibitors targeting oligomers of various amyloid proteins.

Graphical Abstract

*To whom correspondence should be addressed: Zhefeng Guo, Department of Neurology, University of California, Los Angeles, 710 Westwood Plaza, Los Angeles, California 90095, USA. zhefeng@ucla.edu.

AUTHOR CONTRIBUTIONS

AZ, DPB, and EWC designed and carried out experiments, analyzed data, and drafted the manuscript. ZG conceived and supervised the study, designed and carried out the experiments, and drafted the manuscript.

CONFLICTS OF INTEREST

A patent application based on this work is in preparation by University of California, Los Angeles, with Z.G. as the inventor.

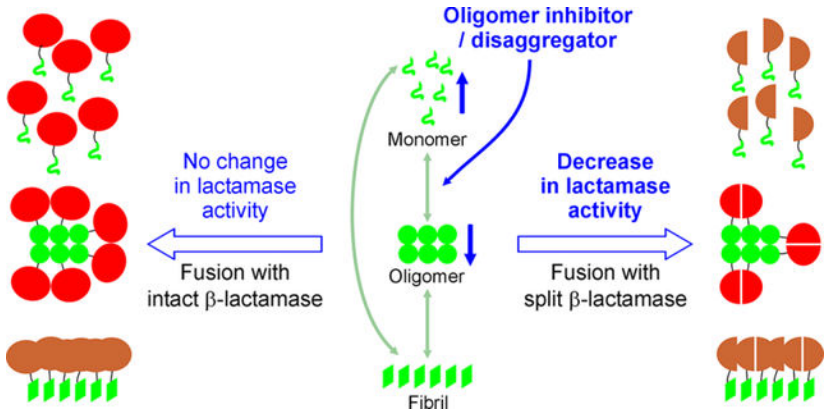

Using a combination of split and intact β-lactamase constructs, we designed a protein aggregation screening platform that can distinguish changes in amyloid oligomers from overall protein aggregation.

INTRODUCTION

Amyloid fibrils resulting from protein aggregation are the pathological hallmarks of a wide range of human disorders including Alzheimer's disease, type 2 diabetes, and Parkinson's disease[1–3]. Although different proteins are involved in different amyloid diseases[4], the amyloids share common features such as binding to thioflavin T[5,6] and cross-β structures[7,8]. Therapeutics targeting amyloids are being actively developed[9]. One example in drug development is US Food and Drug Administration (FDA)-approved monoclonal antibody aducanumab targeting Aβ amyloid fibrils in Alzheimer's disease, although the efficacy of aducanumab has been controversial[10,11]. More recently, Eisai and Biogen reported results from the Phase 3 clinical trials of lecanemab, another anti-Aβ antibody, and showed that it slowed the rate of cognitive decline by 27% over the 18-month trial period[12]. Lecanemab gained accelerated approval from the FDA in early 2023. These encouraging results confirmed the importance of targeting protein aggregation in therapeutic interventions for Alzheimer's and other amyloid-related diseases.

In addition to insoluble amyloid fibrils, protein aggregation, a supersaturation-driven process[13–15], also leads to the formation of soluble aggregates called oligomers. The Aβ oligomers have been shown to cause defects in synaptic transmission[16], decrease long-term potentiation[17], and confer microgliosis[18,19]. Soluble Aβ oligomers can distinguish dementia group from non-dementia individuals when normalized by plaque density[20]. A growing consensus is that Aβ oligomers play a more pathogenic role in Alzheimer's disease than fibrils[21,22]. However, it is challenging to develop assays that specifically target the oligomers. Aβ aggregation is a dynamic process in which different Aβ species, including monomers, oligomers of different sizes and structures, and fibrils, co-exist and inter-convert. As a result, the processes of oligomerization and fibrillization are intertwined and difficult to untangle.

To meet this challenge, we take advantage of the split TEM-1 β-lactamase (BLA) system[23,24], which has been developed to study protein-protein interactions in protein

fragment complementation assays[25–27]. When each half of the split β-lactamase is fused to an Aβ protein, formation of soluble oligomers leads to recovery of β-lactamase activity, while both Aβ monomers and fibrils lose activity because the former is unable to complement the split β-lactamase and the latter sequesters the enzyme in insoluble aggregates. In combination with the aggregation assay using the intact β-lactamase, this aggregation platform allows the distinction between oligomerization and fibrillization.

EXPERIMENTAL

Generation of the intact and split β-lactamase constructs

The TEM-1 β-lactamase gene encoding residues 24–286 was amplified from the pET19b plasmid using PCR. Restriction enzyme recognition sites for NdeI and BamHI were introduced to the 5′- and 3′-end of the β-lactamase sequence via the overhang of the PCR primers. DNA sequence encoding a $(GGGGS)_4$ linker and the Aβ42 protein was chemically synthesized by Integrated DNA Technologies. BclI and XhoI sites were introduced at the 5′- and 3′-end of the $(GGGGS)_4$-Aβ42 sequence during DNA synthesis. The TEM-1 β-lactamase was inserted between the NdeI and BamHI sites of the pET28b plasmid to generate pET28b-BLA. Then the DNA fragment consisting of the $(GGGGS)_4$-Aβ42 sequence was digested with BclI and XhoI, and inserted into the BamHI and XhoI sites of pET28b-BLA to generate pET28b-BLA-$(GGGGS)_4$-Aβ42, which is abbreviated as BLA-Aβ42. The BLA M180T mutation was introduced to the BLA-Aβ42 construct using site-directed mutagenesis. Sanger DNA sequencing was performed to confirm each step of molecular cloning process. The final DNA and protein sequences for the BLA-Aβ42 construct are shown in Figure S1.

To generate the split β-lactamase constructs, deletion mutagenesis was performed using the QuikChange mutagenesis kit (Agilent). For the N-terminal half of the BLA construct (NBLA), residues 196–286 were deleted from the BLA-Aβ42 construct. The final DNA and protein sequences of NBLA-Aβ42 construct are shown in Figure S2. The NBLA-M180T-Aβ42 was generated by performing the same deletion of residues 196–286 from the BLA-M180T-Aβ42 plasmid. The NGR tripeptide insertion mutant of NBLA-Aβ42 was created by including the NGR coding sequence in the PCR primers. The final DNA and protein sequences of NBLA-NGR-Aβ42 are shown in Figure S3. For the C-terminal half of the BLA construct, residues 24–195 of the β-lactamase together with the His-tag sequence between NcoI and NdeI sites were deleted. Then the CBLA-Aβ42 sequence was cut out of pET28b with NcoI and HindIII and inserted to the pCDFDuet-1 plasmid (Millipore Sigma) digested with the same restriction enzymes. The final DNA and protein sequences of CBLA-Aβ42 are shown in Figure S4. DNA sequences of all constructs were confirmed using Sanger sequencing.

The F19D mutation was introduced to the Aβ42 sequence using site-directed mutagenesis and the sequence was confirmed with Sanger sequencing.

The NBLA-M180T construct was generated by performing a deletion mutagenesis to remove Aβ42 sequence from the BLA-M180T-Aβ42 plasmid. The final DNA and protein sequences of NBLA-M180T are shown in Figure S5. To create the CBLA construct, the

CBLA fragment was excised from CBLA-Aβ42 using NcoI/BamHI and inserted to the pCDFDuet-1 plasmid digested with the same restriction enzymes. The final DNA and protein sequences of CBLA are shown in Figure S6.

Growth curve studies of the intact β-lactamase constructs.

The pET28b plasmid containing BLA-Aβ42 constructs were transformed to *E. coli* C41 competent cells (Lucigen). There are two variants of BLA: wild-type (WT) and the M180T mutant. There are also two variants of the Aβ42 protein: WT and the F19D mutant.

For the growth curve studies of BLA-WT fused with either Aβ42 WT or F19D, a single colony was picked to inoculate 20 mL of lysogeny broth (LB) containing 30 μg/mL of kanamycin. The culture was incubated at 37°C with shaking at 220 rpm. The next morning, the cell density of the overnight cultures was determined using optical density at 600 nm (OD_{600nm}). Then the overnight cultures were diluted with LB-kanamycin broth to an OD_{600nm} of 0.35 for both BLA-Aβ42 and BLA-Aβ42-F19D. In a 15-mL tube, we mixed 8 μL of isopropyl-β-D-1-thiogalactopyranoside (IPTG, 0.2 M in deionized water) with 8 mL of diluted cells (OD_{600nm} of 0.35) to achieve the final IPTG concentration of 0.2 mM. We then pipetted 990 μL of these cells to each of the six 1.5-mL microcentrifuge tubes, which were labeled 0, 50, 100, 200, 400, and 800 μg/mL ampicillin. We added 10 μL of deionized water to the 0 μg/mL ampicillin tube, and 10 μL of ampicillin stock solutions at 5, 10, 20, 40, and 80 mg/mL to the tubes labeled 50, 100, 200, 400, and 800 μg/mL ampicillin to achieve the final ampicillin concentration. Different stock ampicillin solutions were made by serial dilutions from the 80 mg/mL solution (in deionized water). We then transferred 50 μL of the cells to a 384-well white microplate with clear bottom (Greiner Bio-One, product number 781095). Each experimental condition consists of four technical repeats. The microplate was sealed with a Breathe-Easy cell culture membrane (Electron Microscopy Sciences, product number 7053610) and incubated in a SpectraMax iD3 microplate reader (Molecular Devices) at 37°C with 1 min of shaking following every 4 min of quiescent incubation. Absorbance at 600 nm was measured every 5 min.

For the growth curve studies of BLA-M180T fused with either Aβ42 WT or F19D, the same procedure for BLA-WT was followed except the final ampicillin concentrations were adjusted to 0, 500, and 1000 μg/mL.

Growth curve studies of the split β-lactamase constructs

For the split β-lactamase constructs, the NBLA-Aβ42 construct on pET28b and the CBLA-Aβ42 construct on pCDFDuet-1 were co-transformed to *E. coli* C41 cells (Lucigen) and selected using kanamycin and streptomycin double resistance. There are four variants of NBLA: NBLA-WT, NBLA-M180T, NBLA-NGR, and NBLA-M180T-NGR. The CBLA fragment of lactamase was not modified. When studying the Aβ42 F19D mutant, the F19D mutation is present in both the NBLA-Aβ42 and CBLA-Aβ42 constructs.

For the growth curve studies of the split β-lactamase constructs, a single colony was picked from the transformation plate to inoculate 20 mL of LB broth containing 30 μg/mL of kanamycin and 50 μg/mL of streptomycin. The culture was incubated at 37°C with shaking at 220 rpm. The next morning, the cells were diluted to an OD_{600nm} of 0.60 using LB-

kanamycin-streptomycin. The rest of the procedure is similarly performed as for the intact β-lactamase constructs with the exception of different ampicillin concentrations as indicated in the results.

Cell lysate preparation

A single colony for the intact β-lactamase construct (BLA-Aβ42), the split β-lactamase-Aβ construct (NBLA-M180T-Aβ42 + CBLA-Aβ42), and the split β-lactamase without Aβ, was used to inoculate 20 mL of LB broth containing the appropriate antibiotics and incubated at 37°C with shaking at 220 rpm. The next morning, 200 μL of the overnight culture was used to inoculate 20 mL of LB broth. IPTG was added to a final concentration of 0.2 mM when the cells grew to an OD_{600nm} of 0.4. The cells were grown for another hour and then pelleted down with centrifugation at 4500 rpm for 20 min. Fresh LB broth was added to the cell pellet and the cells were sonicated on ice using a Branson 450 Sonifier (standard tip, 90% amplitude, pulse mode with 5 s on and 10 s off, 3 min of total on time). An aliquot of the sonicated cell lysate was saved as the total cell lysate. The rest of the cell debris was pelleted by centrifugation (20,000 g, 30 min, 4°C). Ultrafiltration filters with 0.2 μm cutoff were pre-washed by adding 400 μL of water and centrifuged at 14,000 g for 5 min. After removing all the water from the filters, we added 500 μL of the cell lysate supernatant and obtained the 0.2 μm filtrate after centrifugation at 14,000 g at 4°C. Centrifugation was stopped when the volume of the retentate corresponded to the dead volume of the filters. Lactamase activity assays were then performed without delay.

Size exclusion chromatography

A Bio-Rad ENrich SEC 650 10×300 column was used for size exclusion chromatography (SEC) studies of *E. coli* cell lysates. The column was equilibrated with PBS buffer (50 mM phosphate, 140 mM NaCl, pH 7.4), and calibration was performed using the gel filtration standard (Bio-Rad product number 1511901) containing thyroglobulin (670 kD), γ-globulin (158 kD), ovalbumin (44 kD), myoglobin (17 kD), and vitamin B12 (1.35 kD). The sample volume for the gel filtration standard and the cell lysate is 100 and 250 μL, respectively. The flow rate for all chromatography runs was at 1 mL/min. For cell lysate, 0.5 mL fractions were collected for β-lactamase activity assays.

TEM-1 β-lactamase activity assay

Nitrocefin (TOKU-E product number N005, >95% purity) was dissolved in DMSO to obtain a 5 mM stock concentration. Then a 200 μM working solution was prepared in PBS buffer. The TEM-1 β-lactamase activity was determined by mixing 25 μL of the cell lysate with 25 μL of the nitrocefin working solution in a microplate (Greiner Bio-One product number 781095) and measuring the absorbance at 492 nm every min for 10 min using a SpectraMax iD3 microplate reader (Molecular Devices). The lactamase activity assay was performed on: (1) total cell lysate, (2) supernatant after centrifugation to remove cell debris, (3) supernatant filtered through a 0.2 μm ultrafiltration filter, and (4) various SEC fractions. Three technical repeats for each lysate sample were performed. The sample was diluted as needed to obtain the linear range of absorbance change for accurate activity measurements. The β-lactamase activity is represented by the slope of the kinetic measurements, which were obtained using the LINEST function of Microsoft Excel.

RESULTS AND DISCUSSION

Design of a protein aggregation platform based on intact and split β-lactamase constructs

In the aggregation process of Aβ and other amyloid proteins, there are three main aggregated species: monomers, soluble aggregates (mostly oligomers), and insoluble aggregates (mostly fibrils). An effective screening platform distinguishes these three aggregated species, and more importantly, it needs to be able to distinguish the changes in a particular species. The most pressing need is a screening tool that can specifically monitor the changes in Aβ oligomers. To achieve this goal, we utilize a combination of two cell-based and biochemical assays. The first system is a fusion protein of Aβ and intact TEM-1 β-lactamase[28] (Figure 1A). The second is a fusion protein between Aβ and split β-lactamase[23,24] (Figure 1B). TEM-1 β-lactamase is encoded by the ampicillin resistance gene in *E. coli* and other Gram-negative bacteria[29]. The fusion constructs with β-lactamase allow for the use of *E. coli* cell growth or activity assays with cell lysate to screen for aggregation inhibitors or modulators.

The rationale of using the full-length β-lactamase is that formation of insoluble Aβ fibrils will sequester lactamase proteins in the Aβ aggregates and may also cause misfolding of lactamase proteins, and thus reduce the lactamase activity in *E. coli* cells (Figure 1A). As a result, increased Aβ aggregation would lead to reduced lactamase activity and poor cell growth. Previously, Aβ has been fused to reporter proteins such as green fluorescent protein[30] and dihydrofolate reductase[31], and it has been shown that these reporters can be used to monitor Aβ aggregation. Aggregation inhibitors can be screened using the Aβ-lactamase fusion system for changes in the *E. coli* growth curve or lactamase activity. The shortcoming of the intact β-lactamase construct is that Aβ monomers and oligomers are not distinguished because lactamase proteins fused to either are expected to retain activity.

The split lactamase system has one copy of Aβ fused to the N-terminal half of TEM-1 β-lactamase (NBLA), and another copy of Aβ fused to C-terminal half of β-lactamase (CBLA) (Figure 1B). The split β-lactamase system is based on the principle of protein fragment complementation assay, which has been widely used to study protein-protein interactions[25–27]. The activity of β-lactamase is restored only when Aβ proteins interact with each other in soluble oligomers. In fibrils, even though the two halves of β-lactamase can come together, formation of insoluble aggregates would render the enzyme inactive or sequester the enzyme from its substrates.

The combination of the split and intact lactamase constructs can distinguish Aβ oligomer formation from fibrillization. When used for drug screening, inhibitors of Aβ oligomerization would lead to reduced lactamase activity and cell growth for the split β-lactamase constructs. However, increased fibril formation would have the same effect. For the intact β-lactamase construct, only molecules that promote fibrillization would reduce lactamase activity, while oligomer inhibitors would have a muted effect. Therefore, a compound that reduces lactamase activity and cell growth in the split lactamase system, but does not do so in the intact lactamase system, would be a potential drug candidate that specifically inhibits oligomerization.

Intact β-lactamase constructs.

The intact β-lactamase construct consists of residues 24–286 with Aβ42 sequence fused to the C-terminal end via a 20-residue $(GGGGS)_4$ linker (Figure 1A). The first 23 residues of β-lactamase form a signal for secretion to periplasm[32] and are not included in our fusion construct. This allows the fusion protein to be trapped in the cytoplasm. Structural studies have shown that the C-terminal region of Aβ is structured in the amyloid fibrils, while the N-terminal region is more disordered[33–35]. Therefore, the Aβ sequence is placed at the C-terminal end of β-lactamase so that the C-terminal region of Aβ can freely interact with each other during aggregation.

We performed a growth curve study of *E. coli* cells expressing the intact lactamase-Aβ42. The *E. coli* cells were supplemented with IPTG to induce protein expression, and the cell growth was monitored using absorbance measurements at 600 nm in a microplate reader. The cells with 0.2 mM IPTG (Figure 2A, red traces) had similar growth curves as the cells without IPTG (Figure 2A, black traces), suggesting that overexpression of Aβ fusion protein does not have significant effect on cell growth. In the presence of ampicillin, cell density decreased initially and recovered after a lag time (Figure 2A). Eventually, the cell density in the presence of ampicillin reached similar levels as the cells without ampicillin. With increasing concentrations of ampicillin, the cells grew slower and slower, suggesting that the amount of lactamase was in a range sensitive to changes in ampicillin concentrations.

To establish that we can use the changes in growth curve as a proxy for changes in Aβ aggregation, we introduced the F19D mutation to the Aβ42 sequence. Previous studies have shown that the F19D mutation markedly decreased the formation of insoluble Aβ42 fibrils both in vivo and in vitro[31,36–38]. With the F19D mutation, the cell density decreased to a lesser extent than Aβ42 wild-type and the cell growth also recovered faster (Figure 2B). The difference in growth recovery reflects a higher level of lactamase activity in the F19D construct. These results confirm that, with the intact lactamase-Aβ construct, we can use bacterial cell growth as a proxy for Aβ aggregation.

To quantify the effect of ampicillin on cell growth, we defined the “growth recovery time” as the time from the beginning of the decline in cell density to the time when cell density recovers to the same level (Figure 2C, inset). A plot of growth recovery time as a function of ampicillin concentration is shown in Figure 2C. We rationalize that the growth recovery time represents the time needed for the active lactamase to reduce the ampicillin in the culture medium below a growth-permissive concentration threshold. There appears to be a noticeable trend that the difference in growth recovery time between Aβ42 wild-type and F19D mutant increases with increasing concentrations of ampicillin. As a result, using higher concentrations of ampicillin may help detect smaller changes in protein aggregation when performing growth curve studies. Because the cell growth in the presence of ampicillin depends on the total lactamase activity, and because lactamase proteins in both oligomers and monomers are active, the cell growth curve alone does not distinguish contributions from Aβ oligomers or monomers. The relationship between different Aβ aggregates and lactamase activity are further investigated below using size exclusion chromatography of the cell lysates.

To improve our construct, we introduced an M180T mutation to the β-lactamase sequence. The M180T mutation is also referred to as M182T in a numbering system that is based on the consensus sequence of class A β-lactamases[39]. Several previous studies[40–45] show that the M180T mutation suppresses defects of protein folding and improves lactamase stability. Our intent was to see if the M180T mutation would better detect changes in Aβ aggregation. We found that the M180T mutation in β-lactamase dramatically increased the ampicillin resistance of our fusion protein constructs with both wild-type Aβ42 (Figure 3A) and the Aβ42 F19D mutant (Figure 3B). Neither 0.5 or 1 mg/mL ampicillin caused any decrease in cell density. These results suggest that, when an enzyme is used as a reporter of protein aggregation, too much enzyme activity makes it insensitive to changes in protein aggregation. For the intact lactamase construct, the wild-type β-lactamase is more suitable than the M180T mutant to monitor Aβ aggregation.

Split β-lactamase constructs.

For the split β-lactamase constructs, the N- and C-terminal halves of β-lactamase, NBLA and CBLA (Figure 1B), were split between residues 195 and 196 based on the studies of Galarneau et al.[23] and Wehrman et al.[24]. The relative positions of protein of interest and the split lactamase constructs may affect the complementation of enzyme activity. Using GCN4 leucine zippers (ZIP), Galarneau et al.[23] tested various combinations of having the protein of interest at either N- or C-terminal side of NBLA and CBLA. They found that the order of complementation efficiency is NBLA-ZIP / ZIP-CBLA > ZIP-NBLA / ZIP-CBLA > NBLA-ZIP / CBLA-ZIP > ZIP-NBLA / CBLA-ZIP. Wehrman et al.[24] put interacting protein partners at the C-terminal side of NBLA, but N-terminal side of CBLA. In designing the split lactamase-Aβ constructs, our main concern is how the attachment of a fusion protein affects Aβ aggregation. Because the C-terminal end of Aβ is more ordered in Aβ oligomers[46,47] and fibrils[33–35], we chose to put Aβ at the C-terminal side of both NBLA and CBLA constructs so that movement of Aβ C-terminal region is not restricted by the fusion protein.

We performed growth curve studies of *E. coli* cells expressing NBLA-Aβ42 and CBLA-Aβ42. The results showed that the cell growth did not recover within the timeframe of 18 h at ampicillin concentrations of 50 μg/mL or higher (Figure 4A). The cells grew poorly in the presence of 25 μg/mL ampicillin. The poor growth of cells expressing wild-type split lactamase constructs may be due to lower protein expression levels because the cells need to express both NBLA-Aβ42 and CBLA-Aβ42, in comparison with just one protein for the intact lactamase-Aβ42 construct. It is also expected that the split lactamase is less stable than the intact lactamase due to the entropy cost of complementation.

To overcome the low lactamase activity in the split β-lactamase system, we turned to two previously reported constructs of β-lactamase. One is the M180T mutant discussed above. The other construct is the insertion of a tripeptide sequence, NGR, at the C-terminus of NBLA, which was found to increase the activity of the complemented lactamase[24]. In addition, we made an NBLA construct containing both M180T and NGR. Growth curve studies show that the presence of NGR tripeptide did not significantly change the growth curves for the split lactamase-Aβ42 constructs (Figure 4B). The presence of the

M180T mutation, however, led to growth recovery at both 200 and 400 μg/mL ampicillin concentrations (Figure 4C). When both M180T and NGR are introduced to the NBLA construct, the cell growth also recovered at 200 and 400 μg/mL ampicillin (Figure 4D), but with slower recovery than the M180T construct (Figure 4C). Our findings that M180T mutation is critical for good cell growth are in line with previous studies on the split lactamase system showing that the M180T mutation increased the reconstituted lactamase activity 10- to 250-fold over background levels[23].

Next we investigated whether the split β-lactamase constructs can detect the aggregation difference between Aβ42 WT and the F19D mutant. We found that the growth recovery of cells expressing the Aβ42 F19D mutant also requires the M180T mutation in β-lactamase, as both the NBLA-WT (Figure 4A) and NBLA-NGR (Figure 4B) did not lead to cell recovery in the presence of 50 and 100 μg/mL ampicillin. With the NBLA-M180T construct, the Aβ42 F19D mutant had a growth recovery time of 2.6 and 3.8 h with 200 and 400 μg/mL ampicillin, respectively (Figure 4C). In comparison, the growth recovery time for Aβ42 wild-type in the same NBLA-M180T background was 6.1 and 9.0 h with 200 and 400 μg/mL ampicillin, respectively (Figure 4C). The NBLA-M180T-NGR construct also showed that F19D mutation resulted in faster growth recovery compared to wild-type Aβ42 (Figure 4D). Comparing NBLA-M180T-NGR and NBLA-M180T for Aβ42 F19D, the presence of NGR peptide also slowed down cell recovery (Figure 4C, D). However, the NGR construct amplified changes in Aβ aggregation as a result of the F19D mutation. At 200 μg/mL ampicillin, the difference in growth recovery time between Aβ42 WT and F19D is 3.5 h for the M180T construct (Figure 4C), and 5.1h for the M180T-NGR construct (Figure 4D). And this is consistent with previous studies that show NGR improved signal-to-noise ratio in using the split lactamase to study protein-protein interactions[24].

Our results suggest that, when an enzyme is used to report protein aggregation, the enzyme activity needs to be tuned to match the aggregation profile of the amyloid protein. For the intact lactamase construct, wild-type is better at detecting protein aggregation than the M180T mutant because the M180T mutant of β-lactamase is too active (Figures 2 and 3). For the split lactamase construct, the M180T mutant is critical for detecting Aβ aggregation because the wild-type β-lactamase does not provide enough activity (Figure 4). The collection of different β-lactamase constructs provides a toolbox to accommodate the aggregation properties of different amyloid proteins.

Split β-lactamase constructs are sensitive to the formation of soluble Aβ oligomers

To investigate the contribution to β-lactamase activity from Aβ aggregates of different sizes, we studied the cell lysate activity expressing intact and split β-lactamase constructs. Total cell lysate was obtained by sonicating the bacterial cells. The total cell lysate was separated to supernatant and pellet using centrifugation. The supernatant was then filtered through a 0.2 μm ultrafiltration filter to obtain 0.2 μm filtrate. The β-lactamase activity was determined using nitrocefin as a substrate[48]. For both the intact and split β-lactamase constructs (Figure 5), we found that there is no significant difference between total cell lysate, supernatant, and 0.2 μm filtrate, suggesting that the β-lactamase activity exists only in the soluble fraction

of the cell lysate. In other words, formation of insoluble Aβ aggregates leads to loss of β-lactamase activity.

To further investigate whether Aβ forms oligomers in the cell lysate and how oligomer formation contributes to total β-lactamase activity, we fractionated the cell lysate using a Bio-Rad ENrich SEC 650 size exclusion column. Molecular weight calibration was performed using a gel filtration standard containing thyroglobulin (670 kD), γ-globulin (158 kD), ovalbumin (44 kD), myoglobin (17 kD), and vitamin B12 (1.35 kD). Excellent linearity (R^2 = 0.9992) was obtained with the gel filtration standard (Figure S7). We performed β-lactamase activity assays on all protein-containing fractions, ranging from elution volumes of 7–20 mL.

As shown in Figure 6A, the split lactamase-Aβ42 construct shows two main activity peaks, centered at elution volumes of 10.25 and 15 mL. Based on the calibration standard, these two activity peaks have an apparent molecular mass of 600 and 22 kD (Figure S7). The molecular mass of the NBLA-Aβ42 is 27 kD and CBLA-Aβ42 is 16 kD. Therefore, the 600-kD activity peak may contain 14 heterodimers of NBLA-Aβ42 and CBLA-Aβ42, assuming an equal molar mixture in the oligomer. And this corresponds to 28 molecules of Aβ in the 600-kD activity peak. This is consistent with a previous study that shows Aβ42 oligomers consisting of 24–36 subunits[49]. A previous study[50] of Aβ oligomers from Alzhimer's disease brain tissues shows an SEC peak near 158-kD, corresponding to ~35 Aβ molecules. The 22-kD activity peak likely represents a mixture of NBLA-Aβ42 and CBLA-Aβ42, which give an average molecular mass of 21.5 kD. The high level of lactamase activity in the 22-kD activity peak may arise from a high background complementation of the split lactamase, or from the formation of Aβ42 dimers. It is also possible that self-complementation of the split lactamase constructs can drive Aβ dimerization. Aβ dimers have been found in both in vivo[51] and in vitro[52] preparations. Our previous work[53] showed that Aβ forms dimers even in the presence of 8 M urea. The lactamase activity from the 600-kD activity peak accounts for ~20% of total activity in the cell lysate. Therefore, it is a viable option to screen for oligomer-targeting compounds by monitoring lactamase activity in the cell lysate or using cell growth assays.

The intact lactamase-Aβ42 construct also shows two main activity peaks at similar elution volumes (Figure 6B). In contrast to the split lactamase construct, the 22-kD activity peak accounts for 97% of total lysate activity. The much higher activity of the 22-kD activity peak is because the intact lactamase does not require fragment complementation. As a result, changes in the oligomers (600-kD activity peak) would have negligible effect on the total lactamase activity for the intact lactamase construct.

To further characterize the split lactamase construct, we prepared NBLA-M180T and CBLA without Aβ fusion and fractionated the cell lysate using the size exclusion column. As shown in Figure 6C, the split lactamase without Aβ shows only one activity peak near 22 kD. This confirms that NBLA-M180T and CBLA are capable of forming an active lactamase in the absence of Aβ oligomers, representing the background activity in protein fragment complementation assays. The absence of additional activity peaks at higher molecular masses suggests that the 600-kD activity peaks observed in the lactamase-Aβ

fusion construct (Figure 6A) are a result of Aβ aggregation, not driven by lactamase aggregation.

The SEC studies confirmed the design of the split lactamase construct (Figure 1), which is sensitive to the formation of amyloid oligomers. At the same time, the high activity peak at 22-kD suggests high background activity due to spontaneous, in contrast to oligomerization-assisted, complementation of the split lactamase (Figure 6A). This is partly caused by the high level of protein expression in the bacterial expression system. Mutations can be introduced near the binding interface of the split lactamase construct to lower binding affinity, and thus reduce spontaneous complementation. The SEC activity profile described in Figure 6 can be used to evaluate the effects of these mutations in future improvement of the split lactamase construct.

Amyloid oligomers are key drug targets in Alzheimer's disease and other amyloid-related disorders. Due to the difficulty in untangling the processes of oligomerization and fibrillization, few aggregation systems are designed specifically for the screening of oligomer inhibitors. For example, Hecht and co-workers[37] designed a fusion protein construct of Aβ and green fluorescent protein. Aβ aggregation led to reduced fluorescence when overexpressed in *E. coli*, allowing high-throughput screening of aggregation modulators with fluorescence as a readout[30,54]. Liebman and co-workers developed a fusion protein of Aβ and the C-domain of yeast prion Sup35p, a translation termination factor[55]. Aβ aggregation causes ade1–14 gene read-through and allows the yeast cells to grow on medium lacking adenine. As a result, the growth of yeast cells can be used to screen for modulators of Aβ aggregation[56,57]. Stains and co-workers[58] developed a fusion protein construct of Aβ and NanoLuc. Aggregation of Aβ led to reduced bioluminescence, which can be used to screen for aggregation modulators. The Ventura group created a fusion construct using human dihydrofolate reductase and used yeast cell survival as a reporter of protein aggregation[31]. Radford, Brockwell, and co-workers[59] used the refolding of TEM-1 β-lactamase in the periplasm of *E. coli* to screen for aggregation inhibitors. This lactamase system[59] puts the amyloid protein in between the two split lactamase fragments and is fundamentally different from the design of this work. All these systems are based on overall Aβ aggregation, without explicit distinction of fibrillization and oligomerization.

Previously, Hyman and co-workers[49] used a split Gaussia luciferase complementation assay to study Aβ oligomer formation in human cell lines. Using luciferase activity assay, they found that the split luciferase-Aβ fusion formed oligomers corresponding to 24–36 Aβ molecules[49]. This is consistent with our split lactamase-Aβ fusion oligomers that gave an activity peak corresponding to 28 Aβ molecules (Figure 6). Although the luciferase system is a very sensitive assay, Gaussia luciferase displays "flash" kinetics represented by an initial burst of activity and then a rapid decay. The flash properties of Gaussia luciferase has been shown to be caused by covalent inactivation of the enzyme[60]. Because luciferase is not related to cell survival, detecting changes in Aβ aggregation can only be achieved through bioluminescence measurements, limiting the use of the split Gaussia luciferase system in high-throughput screening.

Overall, this work presents a novel protein aggregation platform that combines the use of split and intact β-lactamase to distinguish processes of oligomerization from fibrillization. Changes in the aggregation of amyloid proteins can be monitored through survival of bacterial cells in the presence of ampicillin or lactamase activity assays. For mammalian and other eukaryotic cells, intracellular lactamase activity can be monitored using a membrane-permeable fluorescent substrate[28]. The low-cost assays using bacterial cells are especially suitable for initial high-throughput screening targeting oligomerization of Aβ and other amyloid proteins.

CONCLUSIONS

Aggregation of at least 36 proteins have been identified in a wide range of human disorders[4]. In addition to Aβ, many other amyloid proteins, such as α-synuclein[61,62] and tau[63,64], have also been found to form soluble oligomers that play critical roles in pathogenesis. Identifying small molecule inhibitors or biologics that specifically target the oligomers represent a critical step in developing effective therapeutic interventions. The aggregation reporting platform described in this study can be used to study any amyloid proteins that form intracellular aggregates in *E. coli* or eukaryotic systems. Using *E. coli* cells, both cell growth and lactamase activity in cell lysate can be used to screen for small molecule or biologics inhibitors of oligomerization. While mammalian cells are not subject to the selection pressure exerted by ampicillin, lactamase activity assay can still be performed in live cells using membrane-permeable fluorescent substrates or in cell lysate using nitrocefin. Overall, we expect this aggregation platform to find broad applications in the discovery of aggregation inhibitors for a wide variety of amyloid proteins.

Supplementary Material

Refer to Web version on PubMed Central for supplementary material.

ACKNOWLEDGEMENTS

We thank Lan Duo, Rosemary Wang, Chelsea Jang, and Emilie N. Liu for the technical support of the experiments. This work was supported by the National Institutes of Health (Grant numbers R01AG050687 and R01GM110448)

Abbreviations:

BLA	TEM-1 β-lactamase
WT	wild-type
NBLA	N-terminal half (residues 24–195) of BLA
CBLA	C-terminal half (residues 196–286) of BLA
OD	optical density
IPTG	isopropyl-β-D-1-thiogalactopyranoside
LB	lysogeny broth

SEC	size exclusion chromatography

REFERENCES

1. Sinnige T, Stroobants K, Dobson CM and Vendruscolo M, Q. Rev. Biophys, 2020, 53, e10.
2. Chiti F and Dobson CM, Annu. Rev. Biochem, 2017, 86, 27–68. [PubMed: 28498720]
3. Fitzpatrick AW and Saibil HR, Curr. Opin. Struct. Biol, 2019, 58, 34–42. [PubMed: 31200186]
4. Benson MD, Buxbaum JN, Eisenberg DS, Merlini G, Saraiva MJM, Sekijima Y, Sipe JD and Westermark P, Amyloid, 2020, 1–6. [PubMed: 31766892]
5. Xue C, Lin TY, Chang D and Guo Z, R. Soc. Open Sci, 2017, 4, 160696. [PubMed: 28280572]
6. Groenning M, J. Chem. Biol, 2010, 3, 1–18. [PubMed: 19693614]
7. Gallardo R, Ranson NA and Radford SE, Curr Opin Struct Biol, 2020, 60, 7–16. [PubMed: 31683043]
8. Sawaya MR, Hughes MP, Rodriguez JA, Riek R and Eisenberg DS, Cell, 2021, 184, 4857–4873. [PubMed: 34534463]
9. Cummings J, Lee G, Zhong K, Fonseca J and Taghva K, Alzheimers Dement (N Y), 2021, 7, e12179. [PubMed: 34095440]
10. Knopman DS, Jones DT and Greicius MD, Alzheimers Dement, 2021, 17, 696–701. [PubMed: 33135381]
11. Sabbagh MN and Cummings J, Alzheimers Dement, 2021, 17, 702–703. [PubMed: 33135288]
12. van Dyck CH, Swanson CJ, Aisen P, Bateman RJ, Chen C, Gee M, Kanekiyo M, Li D, Reyderman L, Cohen S, Froelich L, Katayama S, Sabbagh M, Vellas B, Watson D, Dhadda S, Irizarry M, Kramer LD and Iwatsubo T, N Engl J Med, 2023, 388, 9–21. [PubMed: 36449413]
13. Guo Z, Neural Regen Res, 2021, 16, 1562–1563. [PubMed: 33433483]
14. So M, Hall D and Goto Y, Curr. Opin. Struct. Biol, 2016, 36, 32–39. [PubMed: 26774801]
15. Ciryam P, Kundra R, Morimoto RI, Dobson CM and Vendruscolo M, Trends Pharmacol. Sci, 2015, 36, 72–77. [PubMed: 25636813]
16. Zott B, Simon MM, Hong W, Unger F, Chen-Engerer H-J, Frosch MP, Sakmann B, Walsh DM and Konnerth A, Science, 2019, 365, 559–565. [PubMed: 31395777]
17. Li S, Jin M, Koeglsperger T, Shepardson NE, Shankar GM and Selkoe DJ, J Neurosci, 2011, 31, 6627–6638. [PubMed: 21543591]
18. Dhawan G, Floden AM and Combs CK, Neurobiol Aging, 2012, 33, 2247–2261. [PubMed: 22133278]
19. Xu H, Rajsombath MM, Weikop P and Selkoe DJ, EMBO Mol Med, 2018, 10, e8931. [PubMed: 30093491]
20. Esparza TJ, Zhao H, Cirrito JR, Cairns NJ, Bateman RJ, Holtzman DM and Brody DL, Ann. Neurol, 2013, 73, 104–119. [PubMed: 23225543]
21. Benilova I, Karran E and Strooper BD, Nat. Neurosci, 2012, 15, 349–357. [PubMed: 22286176]
22. Haass C and Selkoe DJ, Nat. Rev. Mol. Cell Biol, 2007, 8, 101–112. [PubMed: 17245412]
23. Galarneau A, Primeau M, Trudeau L-E and Michnick SW, Nat Biotechnol, 2002, 20, 619–622. [PubMed: 12042868]
24. Wehrman T, Kleaveland B, Her J-H, Balint RF and Blau HM, Proc Natl Acad Sci U S A, 2002, 99, 3469–3474. [PubMed: 11904411]
25. Blaszczak E, Lazarewicz N, Sudevan A, Wysocki R and Rabut G, Biochem Soc Trans, 2021, 49, 1337–1348. [PubMed: 34156434]
26. Michnick SW, Ear PH, Manderson EN, Remy I and Stefan E, Nat Rev Drug Discov, 2007, 6, 569–582. [PubMed: 17599086]
27. Michnick SW, Landry CR, Levy ED, Diss G, Ear PH, Kowarzyk J, Malleshaiah MK, Messier V and Tchekanda E, Cold Spring Harb Protoc, , DOI:10.1101/pdb.top083543.
28. Zlokarnik G, Negulescu PA, Knapp TE, Mere L, Burres N, Feng L, Whitney M, Roemer K and Tsien RY, Science, 1998, 279, 84–88. [PubMed: 9417030]

29. Sykes RB and Matthew M, Journal of Antimicrobial Chemotherapy, 1976, 2, 115–157. [PubMed: 783110]
30. Kim W, Kim Y, Min J, Kim DJ, Chang Y-T and Hecht MH, ACS Chem Biol, 2006, 1, 461–469. [PubMed: 17168524]
31. Morell M, de Groot NS, Vendrell J, Avilés FX and Ventura S, Mol Biosyst, 2011, 7, 1121–1128. [PubMed: 21240401]
32. Kadonaga JT, Gautier AE, Straus DR, Charles AD, Edge MD and Knowles JR, J. Biol. Chem, 1984, 259, 2149–2154. [PubMed: 6365904]
33. Colvin MT, Silvers R, Ni QZ, Can TV, Sergeyev IV, Rosay M, Donovan KJ, Michael B, Wall JS, Linse S and Griffin RG, J. Am. Chem. Soc, 2016, 138, 9663–9674. [PubMed: 27355699]
34. Xiao Y, Ma B, McElheny D, Parthasarathy S, Long F, Hoshi M, Nussinov R and Ishii Y, Nat. Struct. Mol. Biol, 2015, 22, 499–505. [PubMed: 25938662]
35. Yang Y, Arseni D, Zhang W, Huang M, Lövestam S, Schweighauser M, Kotecha A, Murzin AG, Peak-Chew SY, Macdonald J, Lavenir I, Garringer HJ, Gelpi E, Newell KL, Kovacs GG, Vidal R, Ghetti B, Ryskeldi-Falcon B, Scheres SHW and Goedert M, Science, 2022, 375, 167–172. [PubMed: 35025654]
36. de Groot NS, Aviles FX, Vendrell J and Ventura S, FEBS J, 2006, 273, 658–668. [PubMed: 16420488]
37. Wurth C, Guimard NK and Hecht MH, J. Mol. Biol, 2002, 319, 1279–1290. [PubMed: 12079364]
38. Gray VE, Sitko K, Kameni FZN, Williamson M, Stephany JJ, Hasle N and Fowler DM, G3 (Bethesda), 2019, 9, 3683–3689. [PubMed: 31558564]
39. Ambler RP, Coulson AF, Frère JM, Ghuysen JM, Joris B, Forsman M, Levesque RC, Tiraby G and Waley SG, Biochem J, 1991, 276, 269–270. [PubMed: 2039479]
40. Farzaneh S, Chaibi EB, Peduzzi J, Barthelemy M, Labia R, Blazquez J and Baquero F, Antimicrob Agents Chemother, 1996, 40, 2434–2436. [PubMed: 8891161]
41. Huang W and Palzkill T, Proc Natl Acad Sci U S A, 1997, 94, 8801–8806. [PubMed: 9238058]
42. Zaccolo M and Gherardi E, J Mol Biol, 1999, 285, 775–783. [PubMed: 9878443]
43. Sideraki V, Huang W, Palzkill T and Gilbert HF, Proc Natl Acad Sci U S A, 2001, 98, 283–288. [PubMed: 11114163]
44. Orencia MC, Yoon JS, Ness JE, Stemmer WP and Stevens RC, Nat Struct Biol, 2001, 8, 238–242. [PubMed: 11224569]
45. Wang X, Minasov G and Shoichet BK, J Mol Biol, 2002, 320, 85–95. [PubMed: 12079336]
46. Gu L, Liu C, Stroud JC, Ngo S, Jiang L and Guo Z, J. Biol. Chem, 2014, 289, 27300–27313. [PubMed: 25118290]
47. Ciudad S, Puig E, Botzanowski T, Meigooni M, Arango AS, Do J, Mayzel M, Bayoumi M, Chaignepain S, Maglia G, Cianferani S, Orekhov V, Tajkhorshid E, Bardiaux B and Carulla N, Nat Commun, 2020, 11, 3014. [PubMed: 32541820]
48. Remy I, Ghaddar G and Michnick SW, Nat Protoc, 2007, 2, 2302–2306. [PubMed: 17853887]
49. Hashimoto T, Adams KW, Fan Z, McLean PJ and Hyman BT, J. Biol. Chem, 2011, 286, 27081–27091. [PubMed: 21652708]
50. Savage MJ, Kalinina J, Wolfe A, Tugusheva K, Korn R, Cash-Mason T, Maxwell JW, Hatcher NG, Haugabook SJ, Wu G, Howell BJ, Renger JJ, Shughrue PJ and McCampbell A, J. Neurosci, 2014, 34, 2884–2897. [PubMed: 24553930]
51. McDonald JM, O'Malley TT, Liu W, Mably AJ, Brinkmalm G, Portelius E, Wittbold WM, Frosch MP and Walsh DM, Alzheimers Dement, 2015, 11, 1286–1305. [PubMed: 25846299]
52. Forny-Germano L, e Silva NML, Batista AF, Brito-Moreira J, Gralle M, Boehnke SE, Coe BC, Lablans A, Marques SA, Martinez AMB, Klein WL, Houzel J-C, Ferreira ST, Munoz DP and Felice FGD, J. Neurosci, 2014, 34, 13629–13643. [PubMed: 25297091]
53. Ngo S and Guo Z, Biochem. Biophys. Res. Commun, 2011, 414, 512–516. [PubMed: 21986527]
54. McKoy AF, Chen J, Schupbach T and Hecht MH, J. Biol. Chem, 2012, 287, 38992–39000. [PubMed: 22992731]
55. Bagriantsev S and Liebman S, BMC Biol, 2006, 4, 32. [PubMed: 17002801]

56. Park S-K, Pegan SD, Mesecar AD, Jungbauer LM, LaDu MJ and Liebman SW, Dis Model Mech, 2011, 4, 822–831. [PubMed: 21810907]
57. Park S-K, Ratia K, Ba M, Valencik M and Liebman SW, Microb Cell, 2016, 3, 53–64. [PubMed: 28357335]
58. Zhao J, Nelson TJ, Vu Q, Truong T and Stains CI, ACS Chem Biol, 2016, 11, 132–138. [PubMed: 26492083]
59. Saunders JC, Young LM, Mahood RA, Jackson MP, Revill CH, Foster RJ, Smith DA, Ashcroft AE, Brockwell DJ and Radford SE, Nat Chem Biol, 2016, 12, 94–101. [PubMed: 26656088]
60. Dijkema FM, Nordentoft MK, Didriksen AK, Corneliussen AS, Willemoës M and Winther JR, Protein Sci, 2021, 30, 638–649. [PubMed: 33426745]
61. Chen SW, Drakulic S, Deas E, Ouberai M, Aprile FA, Arranz R, Ness S, Roodveldt C, Guilliams T, De-Genst EJ, Klenerman D, Wood NW, Knowles TPJ, Alfonso C, Rivas G, Abramov AY, Valpuesta JM, Dobson CM and Cremades N, Proc. Natl. Acad. Sci. U.S.A, , DOI:10.1073/pnas.1421204112.
62. Fusco G, Chen SW, Williamson PTF, Cascella R, Perni M, Jarvis JA, Cecchi C, Vendruscolo M, Chiti F, Cremades N, Ying L, Dobson CM and De Simone A, Science, 2017, 358, 1440–1443. [PubMed: 29242346]
63. Gerson JE, Farmer KM, Henson N, Castillo-Carranza DL, Carretero Murillo M, Sengupta U, Barrett A and Kayed R, Mol Neurodegener, 2018, 13, 13. [PubMed: 29544548]
64. Jiang L, Ash PEA, Maziuk BF, Ballance HI, Boudeau S, Abdullatif AA, Orlando M, Petrucelli L, Ikezu T and Wolozin B, Acta Neuropathol, 2019, 137, 259–277. [PubMed: 30465259]

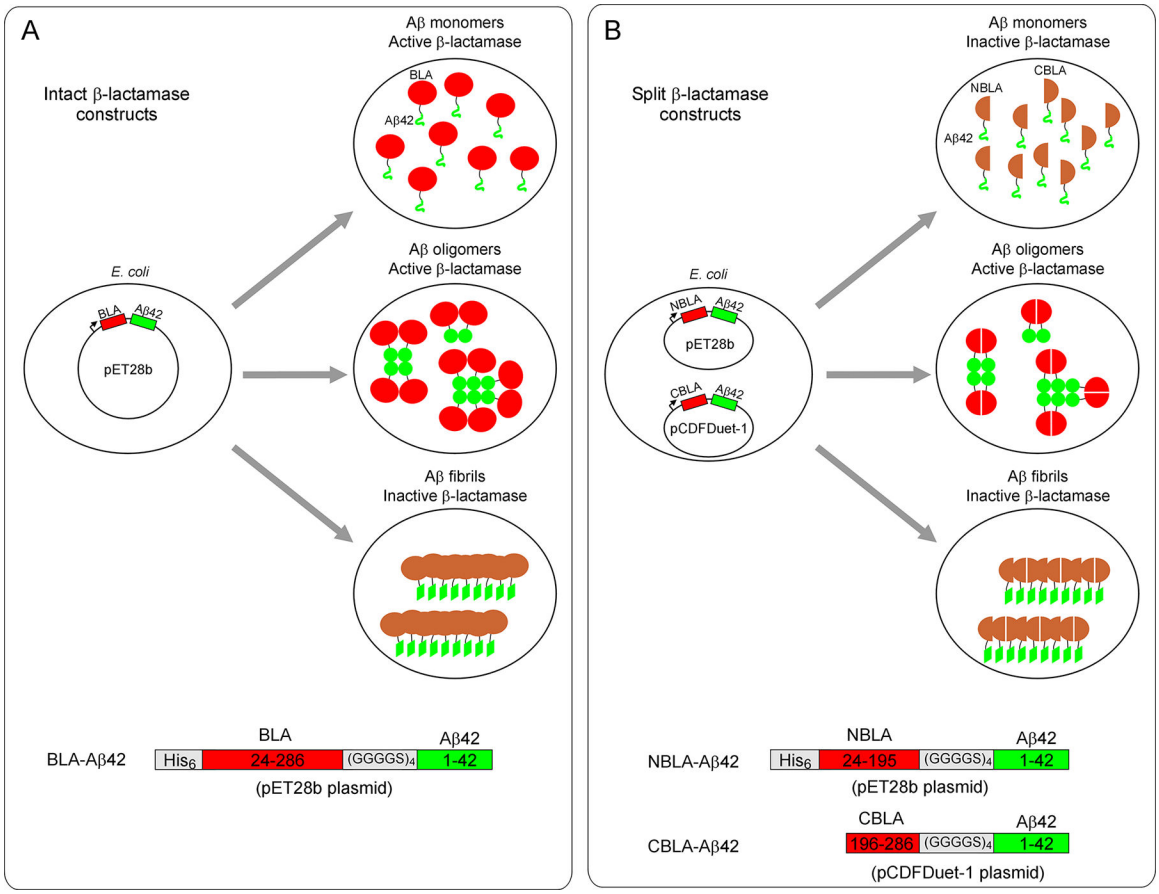

Figure 1. The design of intact and split β-lactamase constructs to study Aβ oligomer and fibril formation.

(A) Fusion protein construct of Aβ and intact β-lactamase (BLA). For the intact β-lactamase construct, lactamase activity exists in both monomers and oligomers. (B) Fusion protein constructs of Aβ and split β-lactamase. For the split construct, lactamase activity exists only in oligomers, not monomers or fibrils.

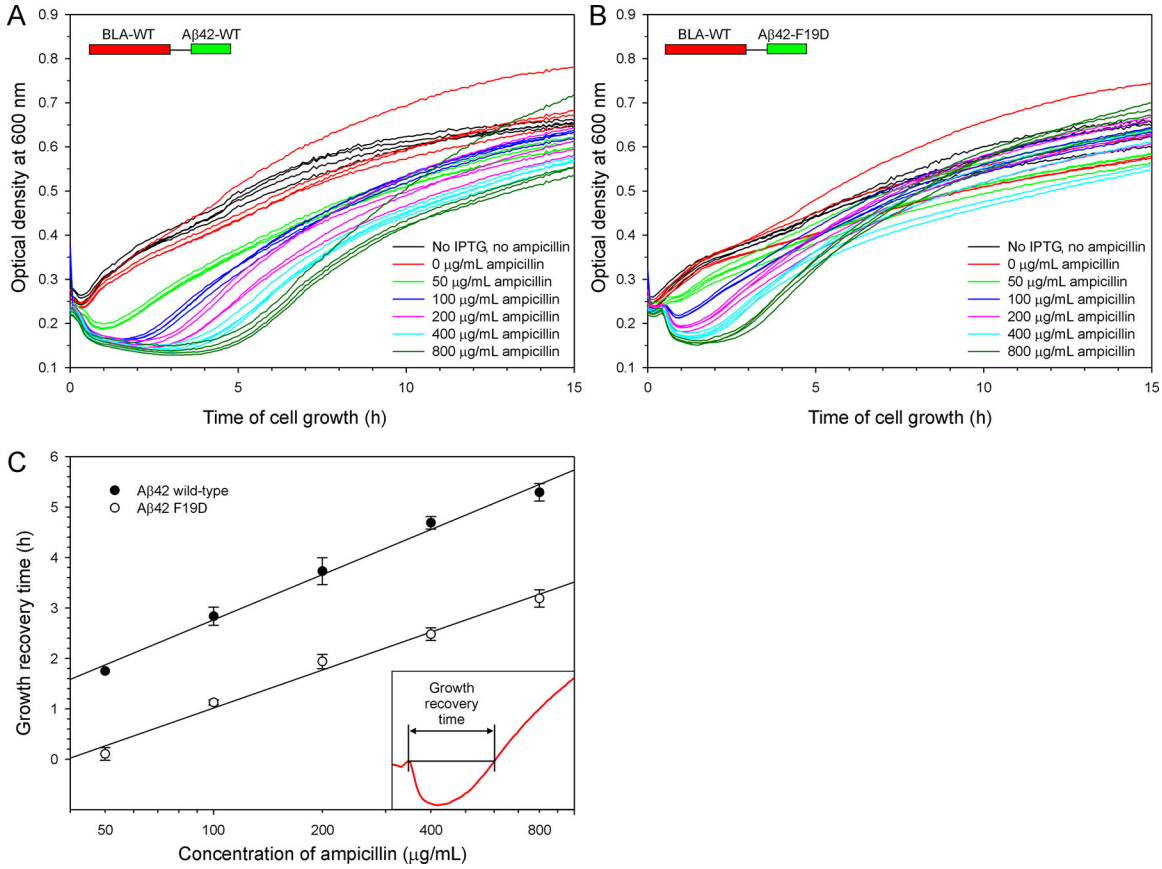

Figure 2. Growth curve studies of the intact β-lactamase constructs.

(A) Fusion with Aβ42 wild-type. (*B*) Fusion with the Aβ42 F19D mutant. *E. coli* cells were grown at 37°C in the presence of 0.2 mM IPTG unless indicated otherwise. (C) Plot of growth recovery time extracted from growth curves as a function of the ampicillin concentration.

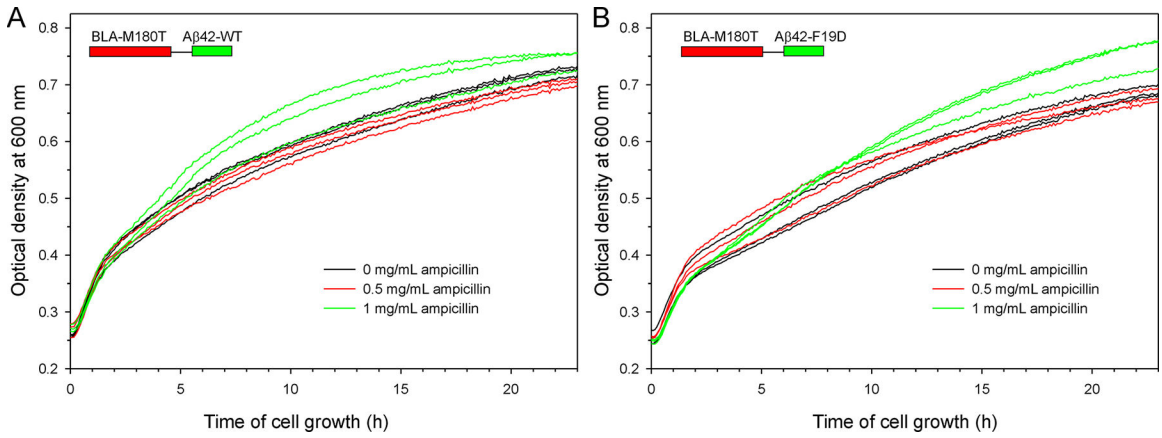

Figure 3. Growth curve studies of the intact β-lactamase construct containing the M180T mutation.

(*A*) Aβ42 wild-type. (*B*) Aβ42 with the F19D mutation. *E. coli* cells were grown at 37°C in the presence of 0.2 mM IPTG and various concentrations of ampicillin as indicated.

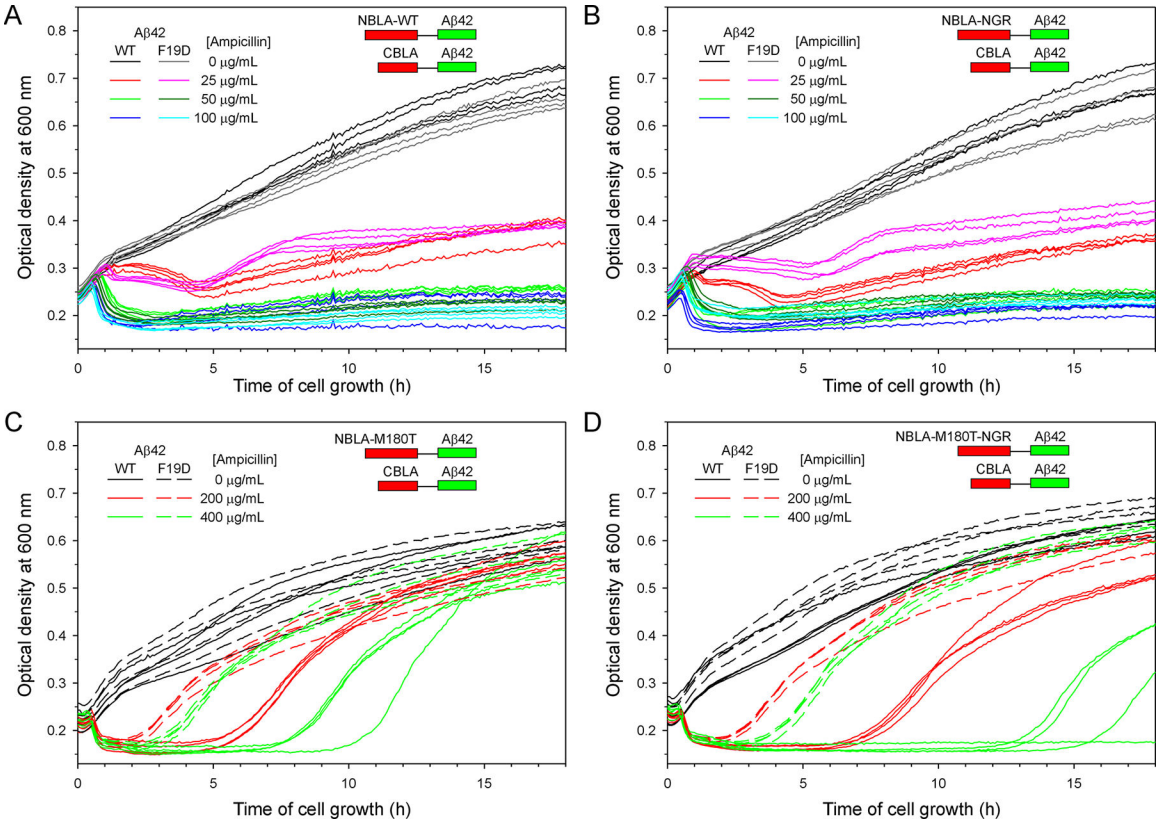

Figure 4. Growth curve studies of the split β-lactamase constructs.

Four different β-lactamase constructs, wild-type (A), insertion of tripeptide NGR (B), M180T (C), and the combination of M18T and NGR (D), were used to express the fusion proteins with either wild-type Aβ42 or the F19D mutant. *E. coli* cells were grown at 37°C in the presence of 0.2 mM IPTG and various concentrations of ampicillin as indicated.

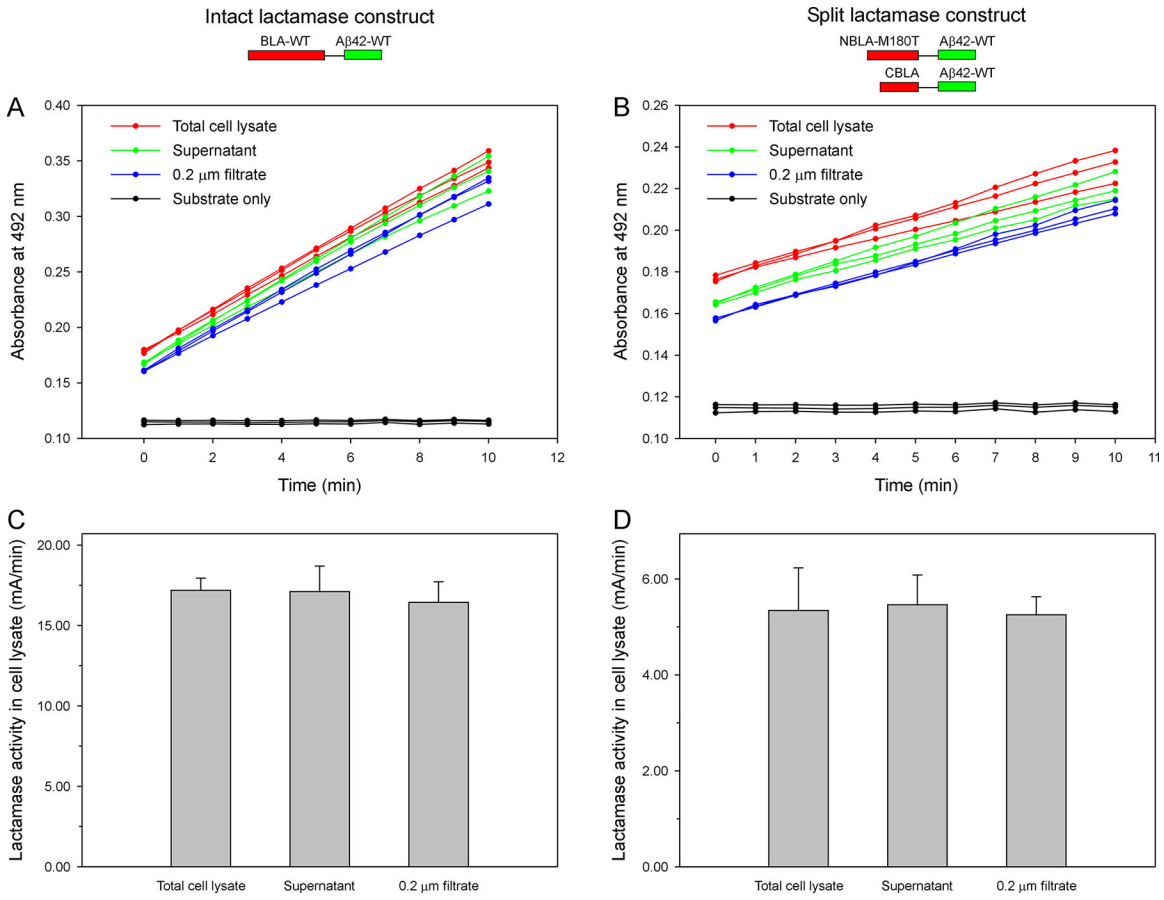

Figure 5. Only soluble fractions of the bacterial cell lysate contain β-lactamase activity.

(A, B) Measurement of β-lactamase activity in *E. coli* cells expressing the intact (A) or split (B) lactamase-Aβ42. Whole cell lysate was centrifuged to separate supernatant from pellet. The supernatant was then filtered through a 0.2 μm ultrafiltration filter to obtain the 0.2 μm filtrate. Nitrocefin was used as the substrate and the activity was measured by monitoring absorbance at 492 nm. The β-lactamase activity was represented as the hydrolysis rate of nitrocefin. (C, D) For both the intact (C) and split (D) lactamase constructs, there are no significant differences between whole cell lysate, supernatant, and 0.2 μm filtrate, suggesting that the lactamase activity is present only in the soluble fraction of the cell lysate. Mean and standard deviation calculated from three technical repeats are shown.

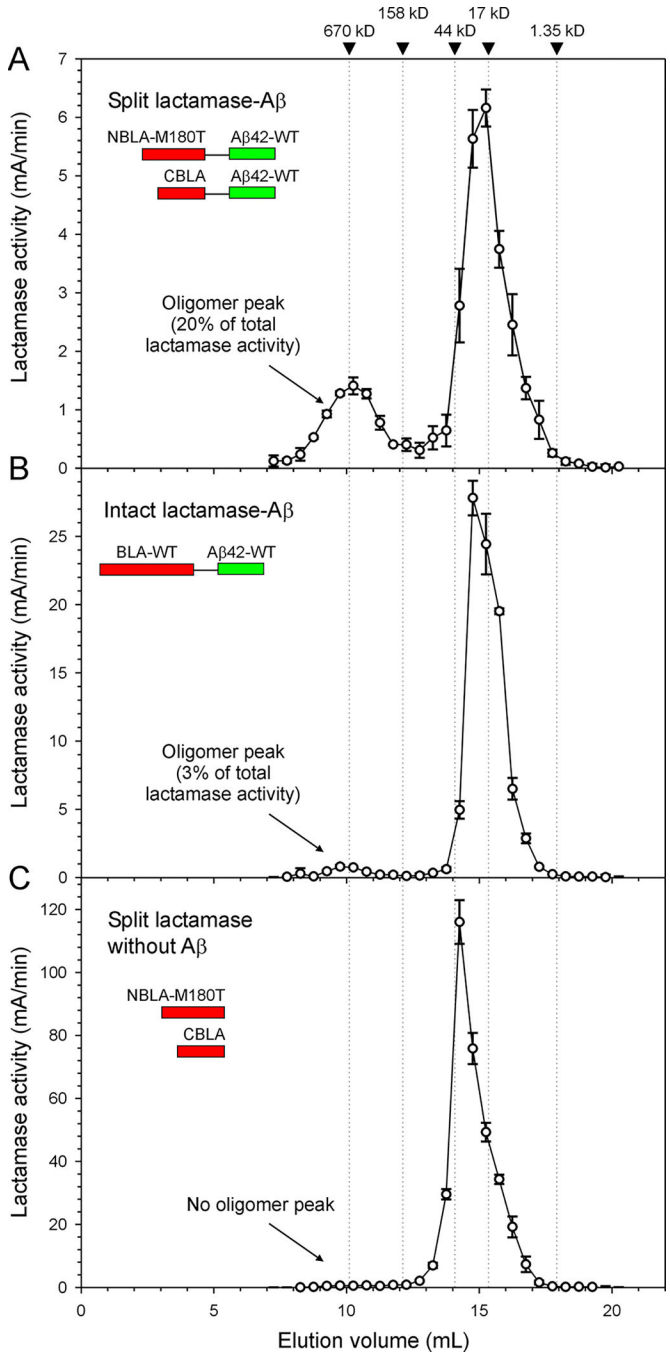

Figure 6. Distribution of β-lactamase activity in bacterial cell lysate fractionated using size exclusion chromatography.

Cell lysate of the split lactamase-Aβ42 (A), intact lactamase-Aβ42 (B), and split lactamase without Aβ (C) was run through an ENrich SEC 650 column, which has a separation size range of 5–650 kD. Fractions were collected between elution volumes of 7 and 20 mL. Lactamase activities were determined for each of these fractions in triplicate. Mean and standard deviations are plotted as a function of elution volume. Arrowheads and vertical lines indicate the peak positions of gel filtration standards. Notably, the split lactamase-Aβ construct shows a significant activity peak corresponding Aβ oligomers of 28 subunits

(A), while the oligomer peak contributes minimally to the total lactamase activity in the intact lactamase-Aβ lysate (B). The split lactamase without Aβ does not show the oligomer peak (C), suggesting that the formation of lactamase-Aβ oligomers is not driven by the aggregation of the split lactamase.